Design of a Hopping Mechanism Using a Voice Coil Actuator: Linear Elastic Actuator in Parallel (LEAP)

Zachary Batts, Joohyung Kim, and Katsu Yamane

***Abstract*— Among legged robots, hopping and running robots are useful because they can traverse terrain at high speeds and are a benchmark platform for locomotion actuators; if an actuator can power a hopping robot, it can power a walking robot. We aim to create a hopping mechanism for a small-scale, one-legged, untethered hopping robot. A parallel-elastic actuator is an efficient way to do this, and enables the actuator to directly inject energy into the spring, but requires a high-speed, low-inertia actuator. Voice coil actuators are electrically-powered direct-drive translational motors that have very low moving inertia, low friction, can produce force at high speeds, and have a linear force output. These qualities make them ideal candidate motors for a linear elastic actuator in parallel ("LEAP"). Here, we derive an electromechanical model of the LEAP mechanism, develop a simple bang-bang hopping controller, and simulate hopping with a range of spring parameters to find an optimal spring stiffness that maximizes hopping height. We detail our implemented design, and characterize its performance through a series of experiments. We test our robot with different spring stiffnesses, and demonstrate hopping at a maximum steady-state of 3.5 cm ground-clearance (approx. 20% leg length). Our results suggest that the LEAP mechanism may serve the weight-bearing functions of a robot leg.**

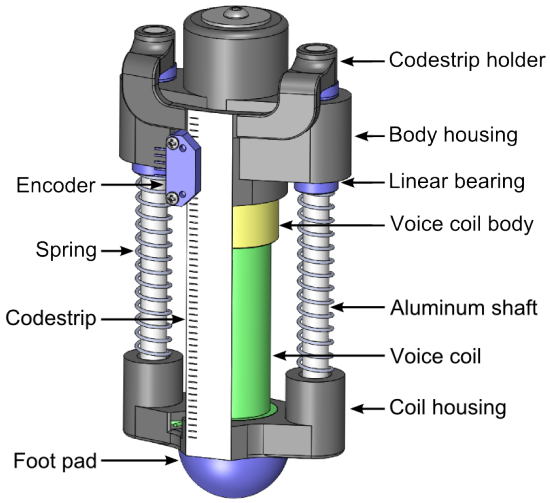

Fig. 1. CAD model of the hopping mechanism. A prismatic joint is realized using two shaft-bearing pairs. Compression springs coil around each shaft and act in parallel to the voice coil. An incremental encoder measures the relative displacement ("stroke") of the coil and body.

I. INTRODUCTION

Legged robots have been conceived and implemented since the 1970s [1], [2]. Hopping robots [3] are highly dynamic mobile platforms that can be represented by reduced-dimensional models [4], which simplifies their control and simulation. However, hopping robots require high-speed, high force actuation due to the physical requirements of achieving non-trivial ground clearance. The first hopping robots were developed at the MIT/CMU Leg Laboratory [5], including a series of 2D and 3D hoppers. More recently, Boston Dynamics has continued this research and produced a quadruped robot, BigDog [6], which can walk and hop robustly using hydraulic actuators. Other researchers [7], [8] have achieved hopping motions with monopod, biped and quadruped robots using electrical motors.

Although untethered hydraulically-actuated hopping robots [6], [9], [10] can often outperform their electrical counterparts, they cause safety concerns and have added design constraints. Hydraulic actuators in a robot system are powered by a compressor, which are relatively large, heavy, and must be placed on the body of the robot. Furthermore, compressors typically operate at high pressure, are often fueled by flammable liquids, and drive very large actuator forces. All of these issues pose safety hazards to human operators, especially during legged locomotion where collisions (wanted and unwanted) are ubiquitous.

Legged robots often employ series elastic actuators (SEA) to drive their joints [11], [12]. By introducing compliance between the actuator and the robot linkage, an SEA is capable of storing energy and absorbing impacts between the robot and the environment. On the other hand, parallel elastic actuators (PEA) can reduce power consumption and increase the net force or torque of the actuator during legged locomotion [13], [14]. Despite these advantages, few prismatic (translational motion) PEAs have been implemented due to the difficulties in converting the rotary motion of an electric motor to linear movement, which can introduce unacceptable friction, hysteresis due to gearing backlash, and non-linear force output. A type of direct-drive linear motor, called a voice coil, may offer an alternative to a geared electric rotary motor. A voice coil is a prismatic electric actuator that has negligible friction, no gearing, and a linear force output [15].

Here, we develop a linear elastic actuator in parallel ("LEAP"), which places a voice coil actuator in parallel with a spring (Fig. 1) to drive a small scale hopping robot. We choose a parallel configuration to offload the force requirements of the mechanism to the spring, and allow the voice coil to inject energy directly into the spring. We first present an electromechanical model of the LEAP mechanism, develop a controller that maximizes energy injection,

Z. Batts, J. Kim, and K. Yamane are with Disney Research, 4720 Forbes Ave., Lower Level, Suite 110, Pittsburgh, PA 15213, USA. {zachary.batts,joohyung.kim,kyamane}@disneyresearch.com

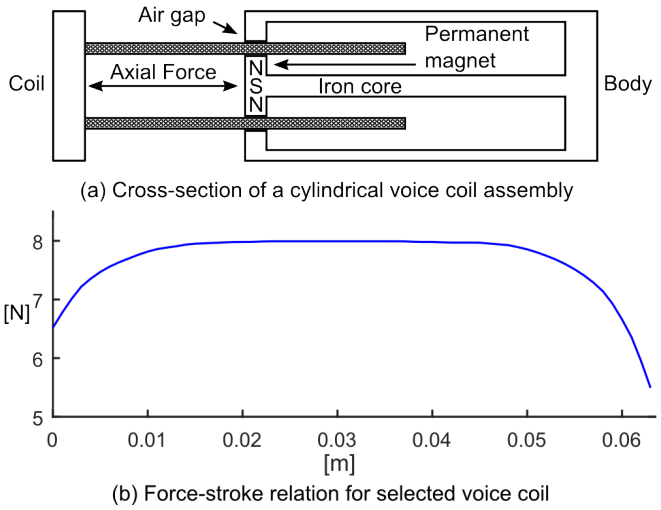

Fig. 2. Physical structure and force-stroke relationship of a voice coil. (a) Cross section of a cylindrical voice coil reveals an iron core that concentrates magnetic flux across a coil. As current is passed through the coil, a force develops between the iron core and coil along their mutual axis. (b) Force-stroke relation for our specific voice coil model [16], at constant current and zero stroke velocity.

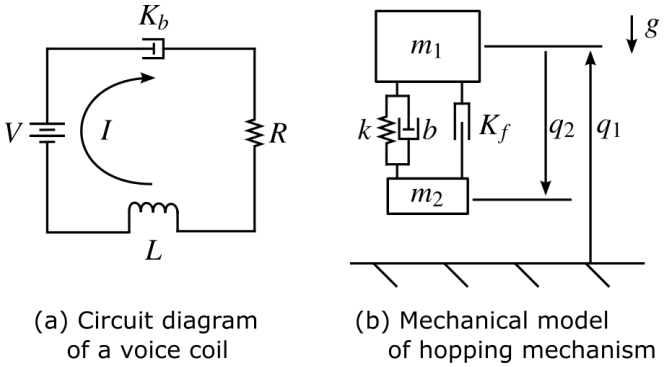

Fig. 3. Electromechanical model diagrams. (a) Voice coil circuit comprises a voltage supply V, back-EMF K_b, resistance R, and inductance L in series, with current I. (b) Two degree-of-freedom mechanical model includes torso mass m_1 with height q_1, voice coil with stroke q_2 and force constant K_f, parallel spring with elasticity k and damping b, foot mass m_2, and gravity g.

and simulate the hopper with a range of spring parameters (Sec. II). We then detail our physical implementation of the LEAP mechanism (Sec. III). Next, we investigate the behavior of our physical system through a series of experiments (Sec. IV); we verify a linear relationship between input current and output force, identify the stiction force of our prismatic joint, and present hopping data for our system at several spring constants. Finally, we discuss our experimental results, summarize the paper, and pose future research (Sec. V).

II. MODEL, CONTROLLER, AND SIMULATION

A. Circuit Model for Voice Coil Dynamics

A voice coil (Fig. 2–A) is an electric actuator that exerts force along its axis that is proportional to the current passing through it. It consists of two components, the body and the coil, that translate relative to each other along their mutual axes, without making physical contact with each other. The body consists of a permanent magnet and iron core that concentrates magnetic flux radially through the coil, perpendicular to its current flow. A magnetic Lorentz force, F, is developed between the body and coil that is proportional to the current through the coil, I, the magnetic flux density, number of windings, and length of conductor [17]. This relation can be condensed to

$$F = K_f I, \tag{1}$$

where K_f is the force constant that is dependent on the relative displacement of the body and coil, called the stroke (Fig. 2–B).

A voice coil circuit (Fig. 3–A) can be modeled as a single loop with voltage source V, resistor R, inductor L, and velocity-dependent electromotive force (back-EMF) element K_b in series. The back-EMF voltage drop is proportional to the stroke velocity. The differential equation governing the electrical dynamics is

$$V - IR - \frac{dI}{dt}L - K_b\frac{dq_2}{dt} = 0, \tag{2}$$

where q_2 is the stroke. K_b has the same dimensions as K_f (in SI units, $K_f = K_b$). Note that the dynamics equations of a voice coil are analogous to a DC rotary motor, except that they describe translational motion. Assuming zero stroke velocity, the relation between current and voltage is first order in time, with RL time constant $\tau = \frac{L}{R}$.

B. Mechanical Model for Parallel Elastic Actuator

Our mechanism comprises an elastic element in parallel with a voice coil (Fig. 3–B) and serves the weight-bearing functions of a leg. Namely, it can produce forces greater than body weight, can support weight when turned off, can act compliantly or rigidly, and can store and dissipate mechanical energy. On its own, a voice coil could not achieve all of these functions. The parallel elastic element reduces the force and power requirements of the voice coil, can store energy, and adds passive compliance to the mechanism. We choose a parallel configuration such that the forces in the elastic element and actuator are additive. Compared to a series-elastic actuator (SEA), a parallel-elastic actuator (PEA) can achieve larger forces and can inject energy into the system during both compression and extension. Both of these qualities are desireable to maximize hopping height. A PEA can also be implemented in a shorter length than an SEA, which means it can have less inertia as a swing leg, and is easier to include in a robot design. We employ a voice coil as our actuator because it has negligible internal friction (the body and coil do not make physical contact), has no gearing, has low moving inertia (a lightweight coil), and has high force bandwidth. These traits mean it can generate net positive work at high speeds and accelerations that are typical during hopping, while passively adding little inertia and friction to the mechanism.

TABLE I

SIMULATION MODEL PARAMETERS AND INITIAL CONDITIONS

Parameter	Value	Units	Parameter	Value	Units
m_1	1.145	kg	R	10	Ω
m_2	0.313	kg	L	3.2	mH
g	9.81	m/s^2	K_f	5	N/A
k_g	14300	N/m	K_b	5	V/m/s
v_{max}	0.01	m/s	V_{max}	22.2	V
$q_1(t=0)$	0.1635	m	l_0	0.0635	m
$q_2(t=0)$	0.0635	m	max(q_2)	0.0635	m
min(q_2)	0	m	q_2^{thresh}	0.0585	m

The equations of motion for our mechanical model can be derived as

$$m_1\ddot{q}_1 = k(l_0 - q_2) - b\dot{q}_2 + K_f I - m_1 g \quad (3)$$

$$m_2(\ddot{q}_1 - \ddot{q}_2) = k(q_2 - l_0) + b\dot{q}_2 - K_f I - m_2 g - F_y, \quad (4)$$

where m_1 and m_2 are the lump masses of the robot torso and foot, respectively, g is the acceleration of gravity, k and b are the spring elastic and damping constants, respectively, l_0 is the spring rest length, q_1 and q_2 are the generalized coordinates (torso height and voice coil stroke), and F_y is the vertical ground reaction force,

$$F_y = -k_g y \left(1 - \frac{\dot{y}}{v_{max}}\right)\left[\frac{\dot{y}}{v_{max}} < 1\right][y < 0], \quad (5)$$

where k_g is the ground stiffness, $y = q_1 - q_2$ is the foot height, $v_{max} > 0$ is the maximum ground relaxation speed, and the $[*]$ operator evaluates to a binary 0 or 1. This nonlinear ground reaction model captures the properties of an inelastic collision ($v_{max} \to 0$ describes perfectly inelastic collisions with infinite damping; $v_{max} = \infty$ describes perfectly elastic collisions) [18]. We use the same contact model to capture mechanical limit collisions at the maximum or minimum stroke (not shown in Equations (3) or (4)).

C. Simple Control Strategy Maximizes Actuator Work

To maximize hopping height, the voice coil should inject maximal energy into the spring during one hopping cycle. To maximize actuator work, we use a simple bang-bang controller that commands zero voltage during flight, maximum negative voltage during compression, and maximum positive voltage during extension. We assume the mechanism is in flight if the stroke exceeds a threshold value $q_2 > q_2^{thresh}$. Similarly, we assume the foot is in contact with the ground if $q_2 \leq q_2^{thresh}$, where there is non-zero spring deflection. Our controller commands voltage as

$$V = \begin{cases} 0 & \text{if } q_2 > q_2^{thresh} \\ -V_{max} & \text{else if } \dot{q}_2 < 0 \\ V_{max} & \text{else if } \dot{q}_2 \geq 0 \end{cases}, \quad (6)$$

where V_{max} is the maximum supply voltage. We don't precompress the spring during flight to avoid exceeding the power limit of the voice coil. Since the RL time constant ($\tau = \frac{L}{R}$) for our voice coil is much smaller than the approximate spring-mass hopping period ($T \approx \sqrt{\frac{m_1}{k}}$), our controller assumes that voltage, current, and force are proportional at any stroke velocity, and that commanding maximum voltage is equivalent to commanding maximum force.

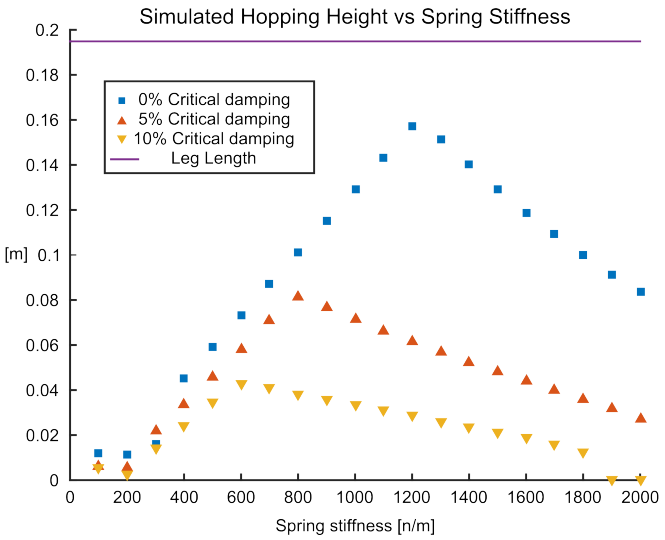

Fig. 4. Average hopping height was recorded for multiple simulations of our system, across a range of spring stiffness and damping coefficients. Critical damping is calculated as $b = 2\sqrt{km_1}$.

We simulate our system continuously (the controller is assumed continuous) with a variable time-step solver (ode15s, relative error tolerance: 1e-4, absolute error tolerance 1e-5) using Matlab Simulink/SimMechanics/Simscape software. To determine an optimal spring stiffness that maximizes hopping height, we simulated our system with a range of stiffnesses, assuming a range of damping coefficients (0%, 5% and 10% critical damping). The simulation parameters and initial conditions given in Table I are equal to the measured parameters of our physical implementation (Sec. III). The force-stroke dependence is given in Figure 2–B; we approximate this relationship as a piecewise function with 10 equally-spaced nodes. We simulate the system for 10 seconds for each trial, with zero initial velocity, and 0.1m initial foot height. The resulting steady-state hopping heights (average ground clearance) are given in Figure 4.

III. PHYSICAL IMPLEMENTATION

Our physical implementation of the hopping mechanism (Fig. 1) centers around an off-the-shelf voice coil motor [16]. Given an approximate desired mass, length, and nominal force for our actuator, we surveyed multiple voice coil manufacturers and selected a model roughly by maximizing work density and stroke while minimizing price. The voice coil parameters are given in Table I, and are the same in simulation and in hardware. The hopping mechanism consists of a torso and a foot assembly, which translate relative to each other via linear bearings and an aluminum shaft. Compression springs coil around each shaft, and act in parallel to the voice coil. An incremental encoder (4724 counts per meter, before quadrature) measures the stroke of the voice coil. A rubber foot pad dampens collisions with the ground. The coil housing, body housing, and codestrip

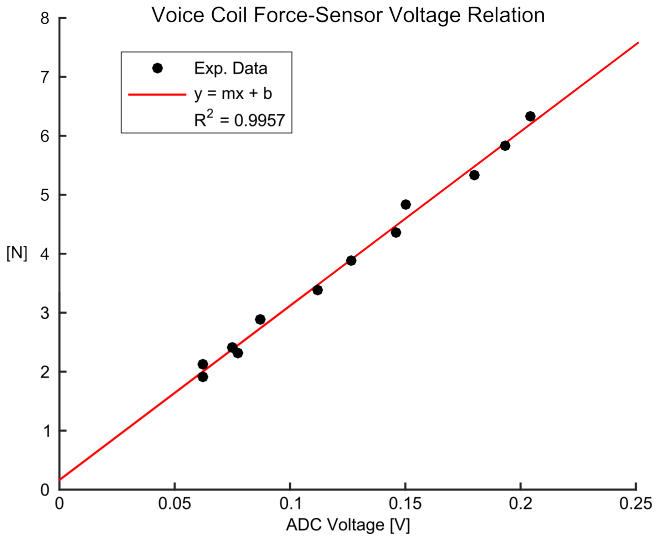

Fig. 5. Linear relation between voice coil force and sensor voltage. Slope and bias for the least-squares linear fit are $m = 29.5$, $b = 0.16$, respectively.

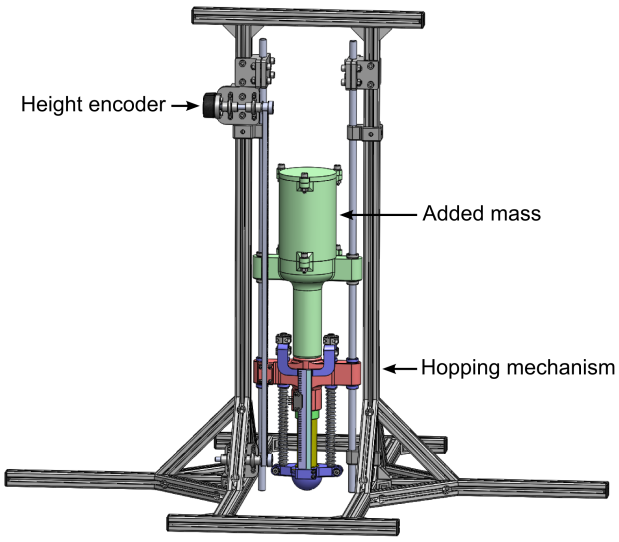

Fig. 6. CAD model of experimental setup. An encoder measures the height of the hopping mechanism, which is constrained to a vertical rail. Mass can be added to the system in measured quantities.

holder were manufactured on a 3D printer. The springs were purchased from stock, and have stiffnesses that roughly span the range of our simulated results.

Since we aim to use our hopping mechanism on an untethered robot, we implemented our controller using embedded electronics, and used lightweight (approx. 210 g total) Lithium-polymer batteries to power our logic circuit and voice coil driver. Our control circuit consists of a microcontroller (Parallax Propeller P8X32A), a voice coil voltage driver (Moticont 800 series), a current sensor (Allegro ACS712) to estimate voice coil force, and an ADC chip (Texas Instruments ADS1015) to read the current sensor. A linear incremental optical encoder (US Digital EM1-0-120-N) and a rotary incremental optical encoder (US Digital E2-32-250-NE-H-D-B) give us full state estimation, and are read directly from the microcontroller. The sensor and control loop run at 1 kHz, while data is output to a desktop computer at approximately 850 Hz (i.e. as fast as possible over serial connection).

IV. EXPERIMENTS

We perform three experiments to identify system parameters and validate our electromechanical model. First, we calibrate our current sensor, ADC, and voice coil to verify a linear relationship between voice coil force and measured current. Second, we identify the breakaway stiction force of our linear bearings using our horizontal experimental setup to ensure that it is small compared to spring and voice coil force. Third, we test our hopping mechanism with different spring stiffnesses and present the results. Through these tests we identify relevant system parameters and show that our original model captures the general behavior of our physical system.

A. *Force-Current Calibration*

In the first experiment, we invert the mechanism such that the foot points upward and rigidly constrains the body housing to a workbench, allowing the foot assembly to translate vertically with a single degree-of-freedom. We remove the springs and add weights of varying mass to the foot assembly to determine a force-current relationship for our voice coil. We run a PID position controller to drive the voice coil to mid-stroke, where we assume the force constant is maximal. We apply a known downward force to the voice coil by accurately measuring the weight of the foot assembly and added mass with a scale. We vary the added mass for each trial and measure the voltage of the current sensor once the position reaches steady-state. We find a linear relation between sensor voltage and applied force ($R^2 = 0.9957$) (Fig. 5). Since the current sensor voltage is proportional to measured current, we verify the linear relation in (1).

B. *Stiction Identification*

In the second experiment, we constrain the body housing horizontally, and remove the springs in order to characterize the friction in the shaft-bearing pairs. We use our PID controller to drive the coil to mid-stroke, then apply zero voltage to the coil. Once the position reaches steady state, we apply a ramp voltage to the coil at approx. $0.04\frac{N}{s}$. We record the voice coil force once the stroke deviates more than 0.6 mm from its steady-state position. We recorded ten trials in either direction (Table II), and found the average breakaway force to be approximately 0.35 N. As we see in Section IV-C, this value is much less than the average voice coil force during hopping, and should have negligible effects on performance.

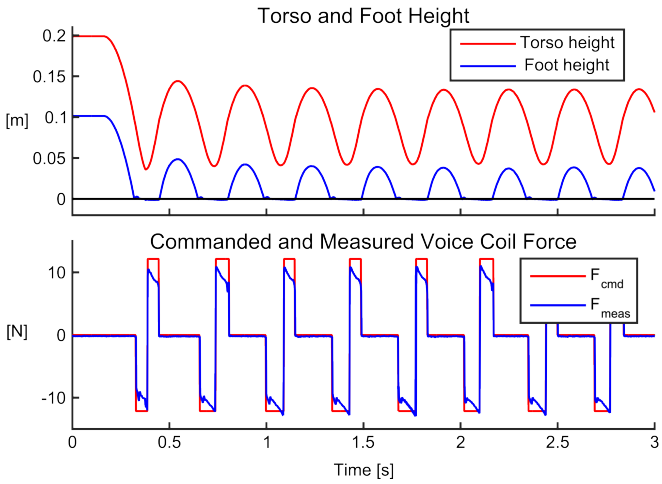

Fig. 7. Selected hopping data collected for a spring stiffness of 771 N/m. (Top) Torso (q_1) and foot height ($q_1 - q_2$) plotted against time. (Bottom) Commanded and measured voice coil force plotted against time.

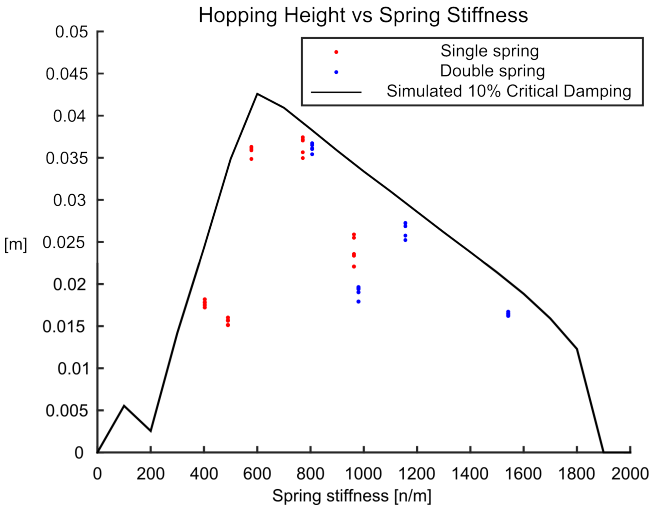

Fig. 8. Experimental hopping height vs stiffness. Average hopping height of the foot is recorded for each trial and plotted against spring stiffness, as given by manufacturer. Stock springs are installed in single or double configuration.

TABLE II

LINEAR BEARING BREAKAWAY STICTION FORCE, IN NEWTONS

Measured force	Average	Measured force	Average
-0.3865		0.3138	
-0.3597		0.3341	
-0.3502		0.3596	
-0.3598		0.3569	
-0.3325		0.3546	
-0.3236	-0.34	0.3599	0.35
-0.3432		0.3720	
-0.3298		0.3563	
-0.3413		0.3633	
-0.3227		0.3636	

C. Hopping Experiment

In our third experiment, we place the hopper on a vertical rail (Fig. 6) to realize our two degree-of-freedom simulation setup. An incremental encoder (788 counts per meter, before quadrature) measures the height of the hopping mechanism. Mass can be added to the torso by placing measured quantities of steel BBs into a container that is rigidly attached to the torso and is also constrained to move along the vertical rail. We install the compression springs of various stiffness around one or both shafts, and run our hopping controller with similar initial conditions as our simulation (approx. 0.1 m foot height). We run 5 trials for each spring stiffness, and record time (t), torso height (q_1), stroke (q_2), commanded voltage (V), and current sensor voltage (V_i). We present data for one selected trial in Figure 7. Snapshots for a different selected trial are shown in Figure 9. For each trial, we record average hopping height of the foot, and plot these values against manufacturer spring stiffness (Fig. 8).

V. DISCUSSION, SUMMARY, AND FUTURE DIRECTION

The experimental data we collected in Sections IV-A and IV-B can be used to design a controller that can precisely and quickly servo voice coil force, especially for applications other than hopping where maximal force output is not always required. For example, a linear controller can be designed using measured current as an input, commanded voltage as an output, and Equations (1)–(4) as plant equations. A feedforward term can augment the linear controller to compensate for the breakaway stiction of the bearings, and might improve performance for trajectories where stroke velocity frequently changes sign.

In Section IV-C, we obtained time series data for hopping that is qualitatively similar to the same data collected in simulation (not shown). When plotted against spring stiffness, average hopping height for our physical system shows a pattern that is similar to our simulated system with 10% critical damping. Both data peak at approximately 600 N/m, and exhibit a similar asymmetric slope to either side of the peak. Yet experimental deviation from our simulated results is most significantly affected by two likely causes. First, in simulation we do not model friction at the q_1 joint, between the torso and world frame, which is present in our experiment due to the linear bearings used to realize the q_1 prismatic joint. Thus, even if our mechanism (i.e. q_2 internal dynamics) were modeled perfectly, the simulation will overestimate hopping height, since it is free from external friction on the torso. Second, the compression springs we purchased have varied material properties, rest lengths, wire diameters, and inner diameters, which affect the frictional characteristics of our mechanism as the spring makes contact with the shaft. Friction is likely inconsistent across springs, not accurately modeled by a parallel spring-dashpot, and not proportional to spring stiffness. A more accurate model might include coulomb friction.

Here, we proposed a novel hopping mechanism which places a voice coil in parallel with an elastic element. We name such a mechanism a linear elastic actuator in parallel ("LEAP"). We modeled our system with a range of spring stiffness and damping parameters, and demonstrated

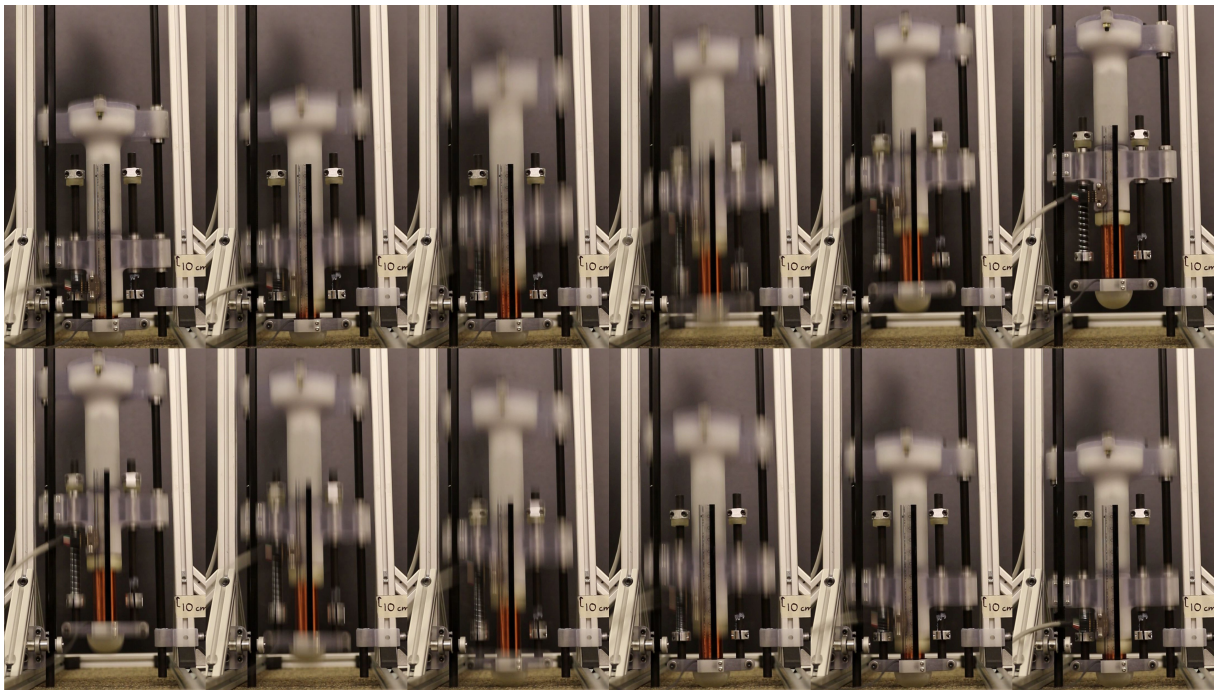

Fig. 9. Snapshots of hopping. Frames are taken at 30 fps, and capture approximately one hopping cycle, from left to right, top to bottom.

a hopping behavior in simulation using a simple bang-bang controller. We implemented a physical prototype that realized the topology of our mechanism and uses embedded power and electronics. We identified a linear force-current relationship, identified breakaway stiction in our bearings, demonstrated hopping along a constrained axis, and showed that our experiment roughly matches our simulated results. We submit that LEAP has many desirable qualities of a general robot leg, and is suitable for dynamic, high-velocity, high-force motions, such as hopping and running. In the future, we plan to use our mechanism in an untethered single-legged hopping robot.

REFERENCES

[1] R. McGhee and G. I. Iswandhi, "Adaptive locomotion of a multilegged robot over rough terrain," *Systems, Man and Cybernetics, IEEE Transactions on*, vol. 9, no. 4, pp. 176–182, April 1979.

[2] S. Sugano and I. Kato, "Wabot-2: Autonomous robot with dexterous finger-arm–finger-arm coordination control in keyboard performance," in *Robotics and Automation. Proceedings. 1987 IEEE International Conference on*, vol. 4, Mar 1987, pp. 90–97.

[3] A. Sayyad, B. Seth, and P. Seshu, "Single-legged hopping robotics research-a review," *Robotica*, vol. 25, no. 05, pp. 587–613, 2007.

[4] W. C. Martin, A. Wu, and H. Geyer, "Robust spring mass model running for a physical bipedal robot," in *Robotics and Automation (ICRA), 2015 IEEE International Conference on*. IEEE, 2015, pp. 6307–6312.

[5] M. H. Raibert, *Legged robots that balance*. MIT press, 1986.

[6] M. Raibert, K. Blankespoor, G. Nelson, R. Playter, *et al.*, "Bigdog, the rough-terrain quadruped robot," in *Proceedings of the 17th World Congress*, vol. 17, no. 1, 2008, pp. 10 822–10 825.

[7] S. Seok, A. Wang, M. Y. Chuah, D. Otten, J. Lang, and S. Kim, "Design principles for highly efficient quadrupeds and implementation on the mit cheetah robot," in *Robotics and Automation (ICRA), 2013 IEEE International Conference on*, May 2013, pp. 3307–3312.

[8] A. De and D. E. Koditschek, "The penn jerboa: A platform for exploring parallel composition of templates," *CoRR*, vol. abs/1502.05347, 2015. [Online]. Available: http://arxiv.org/abs/1502.05347

[9] S. Hyon, T. Emura, and T. Mita, "Dynamics-based control of a one-legged hopping robot," *Proceedings of the Institution of Mechanical Engineers, Part I: Journal of Systems and Control Engineering*, vol. 217, no. 2, pp. 83–98, 2003.

[10] B. Ugurlu, I. Havoutis, C. Semini, and D. Caldwell, "Dynamic trot-walking with the hydraulic quadruped robot x2014; hyq: Analytical trajectory generation and active compliance control," in *Intelligent Robots and Systems (IROS), 2013 IEEE/RSJ International Conference on*, Nov 2013, pp. 6044–6051.

[11] G. Pratt and M. Williamson, "Series elastic actuators," in *Intelligent Robots and Systems 95. 'Human Robot Interaction and Cooperative Robots', Proceedings. 1995 IEEE/RSJ International Conference on*, vol. 1, Aug 1995, pp. 399–406 vol.1.

[12] D. Robinson, J. Pratt, D. Paluska, and G. Pratt, "Series elastic actuator development for a biomimetic walking robot," in *Advanced Intelligent Mechatronics, 1999. Proceedings. 1999 IEEE/ASME International Conference on*, 1999, pp. 561–568.

[13] J. Morrell and J. Salisbury, "Parallel coupled actuators for high performance force control: a micro-macro concept," in *Intelligent Robots and Systems 95. 'Human Robot Interaction and Cooperative Robots', Proceedings. 1995 IEEE/RSJ International Conference on*, vol. 1, Aug 1995, pp. 391–398 vol.1.

[14] S. Wang, W. van Dijk, and H. van der Kooij, "Spring uses in exoskeleton actuation design," in *Rehabilitation Robotics (ICORR), 2011 IEEE International Conference on*, June 2011, pp. 1–6.

[15] J. McBean and C. Breazeal, "Voice coil actuators for human-robot interaction," in *Intelligent Robots and Systems, 2004. (IROS 2004). Proceedings. 2004 IEEE/RSJ International Conference on*, vol. 1, Sept 2004, pp. 852–858 vol.1.

[16] "Linear voice coil motor lvcm-032-076-02," http://www.moticont.com/pdf/lvcm-032-076-02.pdf, accessed: 2015-09-12.

[17] B. Black, M. Lopez, and A. Morcos, "Basics of voice coil actuators," *PCIM-VENTURA CA-*, vol. 19, pp. 44–44, 1993.

[18] H. Geyer and H. Herr, "A muscle-reflex model that encodes principles of legged mechanics produces human walking dynamics and muscle activities," *Neural Systems and Rehabilitation Engineering, IEEE Transactions on*, vol. 18, no. 3, pp. 263–273, 2010.